Applied Numerical Mathematics 81 (2014) 94–104

Contents lists available at ScienceDirect

Applied Numerical Mathematics

www.elsevier.com/locate/apnum

A flux preserving immersed nonconforming finite element method for elliptic problems

Youngmok Jeon [a,∗,1], Do Young Kwak [b]

[a] Department of Mathematics, Ajou University, Suwon 443-749, Republic of Korea
[b] Department of Mathematics, Korea Advanced Institute of Korea, Daejeon, 305-701, Republic of Korea

ARTICLE INFO

Article history:
Received 10 October 2011
Received in revised form 11 October 2013
Accepted 8 November 2013
Available online 27 March 2014

Keywords:
Immersed finite element
Hybridization
Symmetrization

ABSTRACT

An immersed nonconforming finite element method based on the flux continuity on intercell boundaries is introduced. The direct application of flux continuity across the support of basis functions yields a nonsymmetric stiffness system for interface elements. To overcome non-symmetry of the stiffness system we introduce a modification based on the Riesz representation and a local postprocessing to recover local fluxes. This approach yields a P_1 immersed nonconforming finite element method with a slightly different source term from the standard nonconforming finite element method. The recovered numerical flux conserves total flux in arbitrary sub-domain. An optimal rate of convergence in the energy norm is obtained and numerical examples are provided to confirm our analysis.

1. Introduction

In this paper, we consider a simple model interface problem:

$$
\begin{aligned}
&-div\,(\kappa \nabla u) = f \quad \text{in } \Omega, \\
&u = 0 \quad \text{on } \partial\Omega,
\end{aligned}
\tag{1.1}
$$

where the domain $\Omega = \Omega_- \cup \Omega_+$ is a simply connected, bounded polygonal domain with a piecewise smooth interface Γ. The conductivity, κ is piecewise constant so that $\kappa = \kappa_\pm$ on each $\Omega_\pm$.

The finite element (FE) formulation for (1.1) traces back to Babuska et al. [1–3]. They developed the partition of unity FE methods in which the finite elements are constructed by solving the interface problem locally. The local basis functions in these methods are able to capture very well the important features of the exact solution and they can be non-polynomials. Bramble and King derived a finite element method in which the smooth boundary and interface of the problem domain are approximated by polygonal domain and interface [4]. Later, the immersed finite element method (IFE) was introduced, where they allow the interface to cut through the element and the local basis functions constructed to satisfy the interface jump conditions of normal fluxes. IFE methods do not locally solve the interface problem and their basis functions are piecewise polynomials [9,10,14–17].

It is known that the finite volume method produces physically more relevant solutions for evolution equations than the usual finite element does. There have been studies in this direction for interface problems in the name of the immersed

∗ Corresponding author.
E-mail addresses: yjeon@ajou.ac.kr (Y. Jeon), kdy@kaist.ac.kr (D.Y. Kwak).
[1] The research of this author was supported by KRF 2010-0021683.

http://dx.doi.org/10.1016/j.apnum.2013.11.007

finite volume method [8,13]. The purpose of our paper is to introduce a P_1-nonconforming finite element induced by hybridization and a post processing to recover flux conserving numerical fluxes. By hybridization, we mean a construction of the linear system using flux continuity on the support of a local basis function. The major advantage of hybridization is that it produces flux preserving numerical schemes like a finite volume method, however it does not need a control volume generation. For details of hybridized methods we refer to [6,11,12]. As observed in [11,12], the P_1 and P_2 type hybridized methods yield symmetric linear systems for problems without an immersed interface. Especially, for a nonconforming P_1 method the hybridized method results in a symmetric nonconforming finite element system with a modified right hand side. A direct hybridization of immersed finite element method for interface problems yields a nonsymmetric linear system due to the interface elements. Non-symmetry of a linear system can cause difficulties in developing fast convergent iterative schemes.

In this paper we consider a modification of the hybridized method to obtain a symmetric stiffness system. The modification is needed only for elements with an immersed interface. The modification is composed of two procedures: (1) conversion of the nonsymmetric hybridized system into a symmetric nonconforming finite element system by using the Riesz representation, (2) a postprocessing to recover flux by an inverse Riesz representation so that it satisfies intercell flux continuity.

The paper is organized as follows. In Section 2, the function spaces, triangulation and its skeleton, and a hybridization approach are described. In Section 3, a conversion of a hybridized method into a typical nonconforming finite element method by using the Riesz representation is introduced. An analysis in the energy norm is provided in Section 4. In Section 5, we consider the rectangular elements. It is not difficult to see that the analysis in the previous section for triangular elements can be extended directly. In Section 6, we provide numerical results for simple elliptic interface problems by varying conductivity ratio. Numerical experiments are performed for both triangular and rectangular triangulations.

2. Hybridization

Let us first introduce triangulations and functional spaces. Let $\mathcal{T}_h$ be a shape regular, quasi-uniform triangular (or rectangular in Section 5) triangulation of Ω, where $\max_{K\in\mathcal{T}_h} diam(K) = h$. The skeleton K_h of a triangulation $\mathcal{T}_h$ is

$$K_h = \bigcup_{e\in\mathcal{E}_h} e,$$

where $\mathcal{E}_h$ is the set of edges. When the interface Γ trespasses a triangle T, it is called an *(immersed) interface triangle*. Otherwise, it is a noninterface triangle.

Let $H^m(D) = W_2^m(D)$ be the usual Sobolev space of order m with the norm $\|\cdot\|_{m,D}$. Here, $D \subset \mathbb{R}^2$ can be the whole domain Ω or a triangle T. The optimal function space for strong solutions of (1.1) is

$$H^1_{div}(\Omega) = \{u \in H^1(\Omega):\ div(\kappa\nabla u) \in L_2(\Omega)\}.$$

For our numerical purpose we introduce the space $\widetilde{H}^2(D) \subset H^1_{div}(D)$ such that

$$\widetilde{H}^2(D) := \{u \in H^1(D):\ \kappa\nabla u \in [H^1(D)]^2\},$$

equipped with the norm

$$\|u\|^2_{\widetilde{H}^2(D)} := \|u\|^2_{1,D} + \|\kappa\nabla u\|^2_{1,D}.$$

In the finite element analysis we require a regularity of solution

$$\|u\|^2_{H^2(\Omega_+\cup\Omega_-)} = \|u\|^2_{1,\Omega} + \|u\|^2_{2,\Omega_+} + \|u\|^2_{2,\Omega_-} < \infty$$

with the interface condition, $[[\partial^\kappa_\nu u]]_\Gamma = (\kappa_+ \frac{\partial u}{\partial\nu_+} + \kappa_- \frac{\partial u}{\partial\nu_-})|_\Gamma = 0$ to have an optimal order of convergence. However, in our approach we require a stronger regularity $u \in \widetilde{H}_2(\Omega)$ for an optimal convergence analysis.

We denote the skeleton trace of $H^1(\Omega)$ by $H^{1/2}(K_h)$ and that of $H^1_0(\Omega)$ by $H^{1/2}_0(K_h)$. By the nature of nonconforming methods our analysis is based on the discrete Sobolev space $H^1(\mathcal{T}_h) = \prod_{T\in\mathcal{T}_h} H^1(T)$ with the norm and seminorm:

$$\|u\|^2_{1,h} := \sum_{T\in\mathcal{T}_h} \|u\|^2_{1,T}, \qquad |u|^2_{1,h} := \sum_{T\in\mathcal{T}_h} |u|^2_{1,T}.$$

The discrete inner product is given as

$$(\kappa\nabla u, \nabla v)_h = \sum_{T\in\mathcal{T}_h} (\kappa\nabla u, \nabla u)_T.$$

For simplicity of presentation we introduce the notation $A \lesssim B$, which means that $A \leqslant cB$ for some constant $c > 0$, independent of h. Our formulation relies on a simple but fundamental property of the solution of (1.1). Namely, the solution u satisfies the localized problem: for $u \in H^2(\mathcal{T}_h) \cap H^1(\Omega)$,

$$-div\,(\kappa \nabla u) = f \quad \text{in } T$$
$$[[\kappa \nabla u]] := \kappa \frac{\partial u}{\partial \nu} + \kappa' \frac{\partial u}{\partial \nu'} = 0, \quad \text{on } e = \partial T \cap \partial T'. \tag{2.1}$$

From here on, we use the abbreviation, $\partial_\nu^\kappa u := (\kappa \nabla u) \cdot \nu$. The solution u of (2.1) admits locally the following decomposition: with $\lambda = u|_{K_h}$,

$$u = u_\lambda + u^f \quad \text{on } T, \tag{2.2}$$

where the pair (u_λ, u^f) satisfies

$$-div\,(\kappa \nabla u_\lambda) = 0 \quad \text{on } T, \qquad u_\lambda = \lambda \quad \text{on } \partial T \tag{2.3}$$

and

$$-div\left(\kappa \nabla u^f\right) = f \quad \text{on } T, \qquad u^f = 0 \quad \text{on } \partial T, \tag{2.4}$$

respectively. Then u_λ and u^f satisfy the flux continuity equation:

$$\left\langle [[\kappa \nabla u_\lambda]], \mu \right\rangle_{K_h} = -\left\langle \left[\left[\kappa \nabla u^f\right]\right], \mu \right\rangle_{K_h}, \quad \mu \in H_0^{1/2}(K_h). \tag{2.5}$$

The pair $\langle \cdot, \cdot \rangle$ represents the L_2 inner product on K_h or ∂T from here on.

Eqs. (2.2)–(2.5) can be summarized into a hybridized form: find $(u, \lambda) \in \widetilde{H}_0^2(\Omega) \cap H_0^{1/2}(K_h)$ such that

$$-\left(div\,(\kappa \nabla u), w\right)_h + \sum_{T \in \mathcal{T}_h} \left\langle u, \partial_\nu^\kappa w \right\rangle_{\partial T} = (f, w)_h + \sum_{T \in \mathcal{T}_h} \left\langle \lambda, \partial_\nu^\kappa w \right\rangle_{\partial T}, \tag{2.6a}$$

$$\left\langle [[\kappa \nabla u]], \mu \right\rangle_{K_h} = 0 \tag{2.6b}$$

for any $(w, \mu) \in H^1(\mathcal{T}_h) \times H_0^{1/2}(K_h)$. Because of the above formulation we call our approach as a *hybridized method*. For computation and numerical analysis we invoke Eqs. (2.2)–(2.5) rather than the hybridized form (2.6) and it turns out that our method can be analyzed by following the standard finite element analysis of elliptic equations with the unknown u_λ.

3. A nonconforming finite element formulation

Let us introduce local and global immersed finite element spaces. For simplification of our discussion we assume that the interface Γ is a straight line within a triangle. A rationale for this assumption is given in [14].

- If T is not an interface triangle, then the space of local finite elements is defined as

$$\mathcal{W}_T = span\{1, x, y\}, \qquad F = -\frac{1}{4}\left(x^2 + y^2\right).$$

- If T is an interface triangle, assume T is given by $T = S_- \cup S_+$ and $\kappa = \kappa_\pm$ on $S_\pm$ (see Fig. 1) where the interface satisfies the equation $\nu_1 x + \nu_2 y + c = 0$. When $0 < \kappa_+ \leqslant \kappa_-$, the basis for the *immersed finite element* is defined as

$$\mathcal{W}_T = span\{\hat{\phi}_0, \hat{\phi}_1, \hat{\phi}_2\},$$

where

$$\hat{\phi}_0(x, y) = 1, \qquad \hat{\phi}_1(x, y) = -\nu_2 x + \nu_1 y,$$
$$\hat{\phi}_2(x, y) = \begin{cases} \frac{1}{\kappa_-}(\nu_1 x + \nu_2 y + c), & (x, y) \in S_- \\ \frac{1}{\kappa_+}(\nu_1 x + \nu_2 y + c), & (x, y) \in S_+ \end{cases}$$

and

$$F = -\begin{cases} \frac{1}{4\kappa_-}(\nu_1 x + \nu_2 y + c)^2 + \frac{1}{4\kappa_-}(-\nu_2 x + \nu_1 y)^2, & (x, y) \in S_- \\ (\frac{1}{2\kappa_+} - \frac{1}{4\kappa_-})(\nu_1 x + \nu_2 y + c)^2 + \frac{1}{4\kappa_-}(-\nu_2 x + \nu_1 y)^2, & (x, y) \in S_+. \end{cases}$$

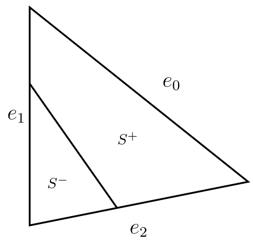

Fig. 1. A reference interface triangle.

When $0 < \kappa_- \leqslant \kappa_+$, the formula for F changes to

$$F = -\begin{cases} (\frac{1}{2\kappa_-} - \frac{1}{4\kappa_+})(\nu_1 x + \nu_2 y + c)^2 + \frac{1}{4\kappa_+}(-\nu_2 x + \nu_1 y)^2, & (x,y) \in S_- \\ \frac{1}{4\kappa_+}(\nu_1 x + \nu_2 y + c)^2 + \frac{1}{4\kappa_+}(-\nu_2 x + \nu_1 y)^2, & (x,y) \in S_+. \end{cases}$$

The basis functions $\{\hat{\phi}_i\}_{i=0}^2$ and F are constructed to satisfy

$$-div\,(\kappa \nabla \hat{\phi}_i) = 0, \qquad -div\,(\kappa \nabla F) = 1 \quad \text{on } T = S_- \cup S_+,$$

together with the normal flux continuity on the interface, $\partial S_- \cap \partial S_+$.

Now, the finite element space is

$$\mathcal{W}_h = \left\{ p \;\middle|\; p \in \bigoplus_{T \in \mathcal{T}_h} \mathcal{W}_T, \int_e p|_T \, ds = \int_e p|_{T'} \, ds,\ e = \partial T \cap \partial T',\ \int_e p|_T \, ds = 0,\ e = \partial T \cap \partial \Omega \right\}.$$

The corresponding interpolation operator is defined as

$$I_h : C(\Omega) \to \mathcal{W}_h, \qquad \int_e (v - I_h v)\, ds = 0, \quad e \subset K_h.$$

The approximation property of this interpolation operator is shown in [14]: for $u \in H^2(\Omega_+ \cup \Omega_-)$

$$\|u - I_h u\|_{0,\Omega} + h\|u - I_h u\|_{1,h} \lesssim h^2 \|u\|_{H^2(\Omega_+ \cup \Omega_-)}, \quad j = 0,\ 1. \tag{3.1}$$

Consider a decomposition of the approximate solution:

$$u_h = v_h + u_h^f \in \mathcal{W}_h,$$

where

$$v_h \in \mathcal{W}_h, \qquad u_h^f = P_0(f)\,(F - I_h F)$$

with $P_0(f) = \frac{1}{|T|}\int_T f\,dx$ for each $T \in \mathcal{T}_h$. It is easy to see that v_h and u_h^f satisfy

$$-div\,(\kappa \nabla v_h) = 0 \quad \text{on } T, \qquad I_h(v_h) = I_h(u_h)$$

and

$$-div\,(\kappa \nabla u_h^f) = P_0(f) \quad \text{on } T, \qquad I_h(u_h^f) = 0,$$

respectively. Moreover, u_h^f has the following estimates:

$$\begin{aligned} &\|u_h^f\|_{0,T} + h\|u_h^f\|_{1,T} \lesssim h^2 \|f\|_{0,T}, \\ &\|u_h^f\|_{\infty,T} + h\|\nabla u_h^f\|_{\infty,T} \lesssim h^2 P_0(f). \end{aligned} \tag{3.2}$$

Hence, v_h and u_h^f solve Eqs. (2.3) and (2.4) approximately.

Then, the hybridized numerical scheme for (2.5) is to find $v_h \in \mathcal{W}_h$ that satisfies

$$\langle [[\kappa \nabla v_h]], \overline{\mu} \rangle_{K_h^0} = -\langle [[\kappa \nabla u_h^f]], \overline{\mu} \rangle_{K_h}, \quad \mu \in \mathcal{W}_h. \tag{3.3}$$

Here, $\overline{\mu}$ is a piecewise constant function on the skeleton K_h such that $\overline{\mu}|_e = \frac{1}{|e|}\int_e \mu\, ds$ for edges $e \subset K_h$.

- If T is not an interface triangle, then ∇v_h is constant on T. Therefore,

$$\langle \partial_\nu^\kappa v_h, \overline{\mu} \rangle_{\partial T} = (\kappa \nabla v_h, \nabla \mu)_T, \quad v_h, \mu \in \mathcal{W}_h.$$

- If T is an interface triangle, ∇v_h is piecewise constant. Therefore,

$$\langle \partial_\nu^\kappa v_h, \overline{\mu} \rangle_{\partial T} \neq (\kappa \nabla v_h, \nabla \mu)_T, \quad v_h, \mu \in \mathcal{W}_h.$$

Hence, Eq. (3.3) does not yield a symmetric discrete system in general. Being nonsymmetric is not desirable since it can cause some difficulties in applying fast convergent iterative numerical schemes such as the conjugate gradient methods and the multigrid methods.

To overcome the nonsymmetric nature of the direct hybridization approach, we consider a modification of (3.3) by introducing the Riesz representation. Let $l_v : \mathcal{W}_h \to \mathbb{R}$ be the linear functional such that $l_v(\mu) = \langle [[\kappa \nabla v]], \overline{\mu} \rangle_{K_h}$. By Riesz representation theorem, there exists a $\sigma_h \in \mathcal{W}_h$ such that

$$(\kappa \nabla \sigma_h, \nabla \mu)_h = l_v(\mu), \quad \mu \in \mathcal{W}_h.$$

Now our scheme is composed of two steps:

Step 1: (Symmetric global solver) Find $\sigma_h \in \mathcal{W}_h$ that satisfies

$$(\kappa \nabla \sigma_h, \nabla \mu)_h = -\langle [[\kappa \nabla u_h^f]], \overline{\mu} \rangle_{K_h}, \quad \mu \in \mathcal{W}_h. \tag{3.4}$$

Step 2: (Local postprocessing) Find $V_h \in \prod_{T \in \mathcal{T}_h} \mathcal{W}_T$ up to a constant on each T such that

$$\langle \partial_\nu^\kappa V_h, \overline{\mu} \rangle_{\partial T} = (\kappa \nabla \sigma_h, \nabla \mu)_T, \quad \mu \in \mathcal{W}_h. \tag{3.5}$$

Remark 3.1.

- Step 2 is introduced to reproduce a globally flux preserving numerical flux $\kappa \nabla V_h$.
- Step 2 is required only when T is an interface triangle. If T is not an interface element we simply have $V_h = \sigma_h$.

Then we use separate forms of numerical solutions for approximation of u and its flux $\Theta = \kappa \nabla u$:

$$U_h := \sigma_h + u_h^f, \qquad \Theta_h := \kappa \nabla V_h + \kappa \nabla u_h^f.$$

The system in (3.4) is the same as the immersed nonconforming finite element formulation in [14] while the right hand side is a bit different. Analysis will show that the numerical solution σ_h has the same convergence property as the immersed nonconforming finite element solution in the energy norm. It is easy to see that the numerical flux $\kappa \nabla V_h$ satisfies

$$\langle [[\kappa \nabla V_h]], 1 \rangle_e = -\langle [[\kappa \nabla u_h^f]], 1 \rangle_e, \quad e \subset K_h.$$

Since $-div\, \Theta_h = P_0(f)$ for each $T \in \mathcal{T}_h$, we have a global flux conservation property:

$$-\int_{\partial D} \Theta_h \cdot \nu \, ds = \int_D f \, dx \tag{3.6}$$

for any subdomain $D = \bigcup_{T \subset D} T$.

For convenience of our analysis we rewrite the modified method (3.4) in a form of the standard immersed nonconforming finite element method:

$$(\kappa \nabla \sigma_h, \nabla \mu)_h = \left(P_0(f), \mu\right)_\Omega - \left(\kappa \nabla u_h^f, \nabla \mu\right)_h + \sum_{T \in \mathcal{T}_h} \langle \partial_\nu^\kappa u_h^f, \mu - \overline{\mu} \rangle_{\partial T}, \quad \mu \in \mathcal{W}_h. \tag{3.7}$$

4. Convergence analysis

We begin this section by introducing the well-known theorems, see [5,7].

Lemma 4.1. *For $u \in H^1(T)$,*

$$\|u\|_{\partial T} \lesssim \left(\frac{1}{h} \|u\|_{0,T}^2 + h|u|_{1,T}^2 \right)^{1/2}. \tag{4.1}$$

Corollary 4.2. *Let e be an edge of T and $T = S_+ \cup S_-$. Then,*

$$\|u - \bar{u}\|_{\partial T} \lesssim h^{1/2}|u|_{1,T}$$

and

$$\left|\int_e \phi(v - \bar{v})\,ds\right| \lesssim h|\phi|_{1,T}|v|_{1,T}$$

for $u \in H^1(T)$.

Proof. Using $\bar{u} = \overline{I_h u}$ and the inverse estimate $h|\nabla I_h u|_{1,S_+\cup S_-} \lesssim \|\nabla I_h u\|_{0,T}$,

$$\begin{aligned}
\|u - \bar{u}\|_{\partial T} &\lesssim \|u - I_h u\|_{0,\partial T} + \|I_h u - \overline{I_h u}\|_{0,\partial T} \\
&\lesssim h^{1/2}\|\nabla u\|_{0,T} + h\|\nabla I_h u\|_{0,\partial T} \\
&\lesssim h^{1/2}\|\nabla u\|_{0,T} + h\big(\|\nabla I_h u\|_{0,\partial S_+} + \|\nabla I_h u\|_{0,\partial S_-}\big) \\
&\lesssim h^{1/2}\|\nabla u\|_{0,T} + h\left(\frac{1}{h}\|\nabla I_h u\|^2_{0,S_+\cup S_-} + h|\nabla I_h u|^2_{1,S_+\cup S_-}\right)^{1/2} \\
&\lesssim h^{1/2}\|\nabla u\|_{0,T}.
\end{aligned}$$

Here, $\|u\|_{t,S_+\cup S_-} = \|u\|_{t,S_+} + \|u\|_{t,S_-}$ for $t = 0, 1$. We have the first estimate. The second estimate follows immediately. □

The following theorem states the energy norm estimate of the nonconforming finite element solution in (3.4) (equivalently, (3.7)).

Theorem 4.3. *Suppose u is the exact solution and σ_h is the finite element solution of the symmetric nonconforming method (3.4). Then we have the following error estimate.*

$$\|u - \sigma_h\|_{1,h} \lesssim h\big(\|f\|_{0,\Omega} + \|u\|_{\widetilde{H}^2(\Omega)}\big)$$

for $u \in \tilde{H}^2(\Omega)$ and $f \in H^0(\Omega)$.

Proof. The exact solution u satisfies $\langle[[\kappa\nabla u]], \overline{\mu}\rangle_{K_h} = 0$ for $\mu \in \mathcal{W}_h$. Then,

$$\sum_{T\in\mathcal{T}_h}\langle\partial_\nu^\kappa u, \mu\rangle_{\partial T} = \sum_{T\in\mathcal{T}_h}\langle\partial_\nu^\kappa u, \mu - \overline{\mu}\rangle_{\partial T}. \tag{4.2}$$

The integration by parts yields that

$$(\kappa\nabla u, \nabla\mu)_h = (f, \mu) + \sum_{T\in\mathcal{T}_h}\langle\partial_\nu^\kappa u, \mu - \overline{\mu}\rangle_{\partial T}. \tag{4.3}$$

Subtracting (4.2) from (3.7) and subtracting $I_h u$ from both sides, we have

$$\begin{aligned}
\big(\kappa\nabla(\sigma_h - I_h u), \nabla\mu\big)_h &= \big(\kappa\nabla(u - I_h u), \nabla\mu\big)_h + \big(P_0(f) - f, \mu\big)_\Omega - \big(\kappa\nabla u_h^f, \nabla\mu\big)_h \\
&\quad + \sum_{T\in\mathcal{T}_h}\langle\partial_\nu^\kappa u_h^f, \mu - \overline{\mu}\rangle_{\partial T} - \sum_{T\in\mathcal{T}_h}\langle\partial_\nu^\kappa u, \mu - \overline{\mu}\rangle_{\partial T} \\
&= E_1 + E_2 + E_3 + E_4 + E_5.
\end{aligned} \tag{4.4}$$

Simple calculation with Corollary 4.2 yields

$$\begin{aligned}
|E_1| &= \big|\big(\kappa\nabla(u - I_h u), \nabla\mu\big)_h\big| \lesssim h\|u\|_{\widetilde{H}^2(\Omega)}|\mu|_{1,h}, \\
|E_2| &= \big|\big(P_0(f) - f, \mu\big)_h\big| = \big|\big(f, \mu - P_0(\mu)\big)_h\big| \lesssim h\|f\|_{0,\Omega}|\mu|_{1,h}, \\
|E_3| &= \big|\big(\kappa\nabla u_h^f, \nabla\mu\big)_h\big| \lesssim h\|f\|_{0,\Omega}|\mu|_{1,h}, \\
|E_4| &= \left|\sum_{T\in\mathcal{T}_h}\langle\partial_\nu^\kappa u_h^f, \mu - \overline{\mu}\rangle_{\partial T}\right|
\end{aligned}$$

$$\lesssim \sum_{T\in\mathcal{T}_h} h\big|P_0(f)\big| \int_{\partial T} |\mu-\overline{\mu}|\,ds$$
$$\lesssim \sum_{T\in\mathcal{T}_h} h^{1/2}\|f\|_{0,T}\|\mu-\overline{\mu}\|_{0,\partial T}$$
$$\lesssim h\|f\|_{0,\Omega}|\mu|_{1,h}.$$

Using continuity of $\partial_\nu^\kappa u$ on the intercell boundaries,

$$|E_5| = \left|\sum_{T\in\mathcal{T}_h}\langle\partial_\nu^\kappa u, \mu-\overline{\mu}\rangle_{\partial T}\right|$$
$$= \left|\sum_{T\in\mathcal{T}_h}\langle\partial_\nu^\kappa u - \overline{\partial_\nu^\kappa u}, \mu-\overline{\mu}\rangle_{\partial T}\right|$$
$$= \sum_{T\in\mathcal{T}_h} h\|\kappa\nabla u\|_{1,T}\|\nabla\mu\|_{0,T} \lesssim h\|u\|_{\widetilde{H}^2(\Omega)}|\mu|_{1,h}.$$

The theorem is proved. □

Now, we investigate the convergence property of the post-processed solution V_h.

Theorem 4.4. *The flux recovery formula,*

$$\langle\partial_\nu^\kappa V_h, \overline{\mu}\rangle_{\partial T} = (\kappa\nabla\sigma_h, \nabla\mu)_T, \quad \mu\in\mathcal{W}_T, \tag{4.5}$$

is uniquely solvable for $V_h\in\mathcal{W}_T$ up to a constant for a given $\sigma_h\in\mathcal{W}_T$. Suppose σ_h is the solution of (3.4) (equivalently, (3.7)). Then, the following error estimate holds:

$$|u-V_h|_{1,T} \lesssim h\big(\|u\|_{\widetilde{H}^2(T)} + \|f\|_{0,T}\big).$$

Proof. Let us consider a space, $\overset{o}{\mathcal{W}}_T = span\{\hat{\phi}_1 - P_0(\hat{\phi}_1),\ \hat{\phi}_2 - P_0(\hat{\phi}_2)\}$. By the Riesz representation, there exists a mapping $\mathcal{S}:\overset{o}{\mathcal{W}}_T\to\overset{o}{\mathcal{W}}_T$ such that $\mathcal{S}(V_h) = \sigma_h - P_0(\sigma_h)$ in (4.5). It is easy to see that the matrix representation of $\mathcal{S}$ is a nonsingular 2×2 matrix. Hence, Eq. (4.5) is uniquely solvable for V_h in $\overset{o}{\mathcal{W}}_h$. Then, $|\mathcal{S}u|_{1,T}$ and $|u|_{1,T}$ are norms in $\overset{o}{\mathcal{W}}_h$. Using the scale invariance, we can see that two norms are equivalent: $c_1|\mathcal{S}u|_{1,T}\leqslant|u|_{1,T}\leqslant c_2|\mathcal{S}u|_{1,T}$ for $u\in\overset{o}{\mathcal{W}}_T$, where $c_1, c_2>0$ are constants independent of the size and shape of T for a shape regular triangulation.

Let us turn to the error analysis. The interpolation $I_h u$ satisfies

$$\langle\partial_\nu^\kappa I_h u, \overline{w}\rangle_{\partial T} = (\kappa\nabla I_h u, \nabla w)_T + \langle\partial_\nu^\kappa I_h u, \overline{w}-w\rangle_{\partial T}, \quad w\in\mathcal{W}_T$$
$$= (\kappa\nabla I_h u, \nabla w)_T + \langle\partial_\nu^\kappa(I_h u - u), \overline{w}-w\rangle_{\partial T} + \langle\partial_\nu^\kappa u, \overline{w}-w\rangle_{\partial T}.$$

Subtraction of the above equation from (4.5) yields

$$\langle\partial_\nu^\kappa(V_h - I_h u), \overline{w}\rangle_{\partial T} = \big(\kappa\nabla(\sigma_h - I_h u), \nabla w\big)_T - \langle\partial_\nu^\kappa(I_h u - u), \overline{w}-w\rangle_{\partial T} - \langle\partial_\nu^\kappa u, \overline{w}-w\rangle_{\partial T}$$
$$= E_1 + E_2 + E_3.$$

Using the approximation property of σ_h (Theorem 4.3) and $I_h u$ (see (3.1)),

$$|E_1| = \big|\big(\kappa\nabla(\sigma_h - I_h u), \nabla w\big)_T\big| \lesssim h\big(\|u\|_{\widetilde{H}^2(T)} + \|f\|_{0,T}\big)|w|_{1,T}.$$

We need some care for the estimate of E_2 when $T = S_-\cup S_+$ since $I_h u\notin\widetilde{H}^2(T)$. First we extend the definition of $\overline{w}$ so that it is defined on the part of interface $\partial S_-\cap\partial S_+$ also. Since $\partial_\nu^\kappa(I_h u - u)$ is continuous on $\partial S_-\cap\partial S_+$, we have by the approximation property of $I_h u$,

$$|E_2| = \big|\langle\partial_\nu^\kappa(u - I_h u), \overline{w}-w\rangle_{\partial T}\big|$$
$$= \big|\langle\partial_\nu^\kappa(u - I_h u), \overline{w}-w\rangle_{\partial S_-} + \langle\partial_\nu^\kappa(u - I_h u), \overline{w}-w\rangle_{\partial S_+}\big|$$
$$\lesssim \big|\langle\partial_\nu^\kappa(u - I_h u), \overline{w}-w\rangle_{\partial S_-}\big| + \big|\langle\partial_\nu^\kappa(u - I_h u), \overline{w}-w\rangle_{\partial S_+}\big|$$
$$\lesssim \big\|\kappa\nabla(u - I_h u)\big\|_{0,\partial S_-}\|w-\overline{w}\|_{0,\partial S_-} + \big\|\kappa\nabla(u - I_h u)\big\|_{0,\partial S_+}\|w-\overline{w}\|_{0,\partial S_+}$$

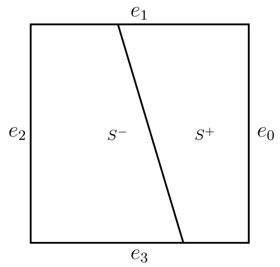

Fig. 2. A reference interface rectangle.

$$\lesssim \left(\frac{1}{h}\left\|\kappa\nabla(u-I_hu)\right\|^2_{0,S_-\cup S_+}+h\left\|\kappa\nabla(u-I_hu)\right\|^2_{1,S_-\cup S_+}\right)^{1/2}\left(\|w-\overline{w}\|_{0,\partial T}+\|w-\overline{w}\|_{0,\Gamma\cap T}\right)$$
$$\lesssim h|u|_{\widetilde{H}^2(T)}|w|_{1,T}.$$

As the proof of E_5 in Theorem 4.3,

$$|E_3|=\left|\langle\partial^\kappa_\nu u,\overline{w}-w\rangle_{\partial T}\right|$$
$$\lesssim h|u|_{\widetilde{H}^2(T)}|w|_{1,T}.$$

As a result, we have

$$|V_h-I_hu|_{1,T}\lesssim h\left(\|u\|_{\widetilde{H}^2(T)}+\|f\|_{0,T}\right).$$

From this and the interpolation property, the theorem is immediate. □

As a result of the above theorems and the estimate for u_h^f in (3.2), we have

$$\|\Theta-\Theta_h\|_{0,h}\lesssim h\left(\|u\|_{\widetilde{H}^2(T)}+\|f\|_{0,T}\right).$$

5. Rectangular elements

In this section we introduce rectangular elements. It is easy to see that the same kind of analysis in the previous section for triangular meshes is applicable to rectangular meshes.

Let us firstly introduce the local rectangular elements.

- When T is not an interface rectangle, the local finite element space is
$$\mathcal{W}_T=span\left\{1,x,y,\left(x^2-y^2\right)\right\}.$$
- When $T=S_-\cup S_+(\kappa=\kappa_\pm \text{ on } S_\pm)$ is an interface rectangle (Fig. 2) with the interface, $\nu_1x+\nu_2y+c=0$, the local finite element space is
$$\mathcal{W}_T=span\left\{\hat{\phi}_0,\hat{\phi}_1,\hat{\phi}_2,\hat{\phi}_3^\alpha\right\},$$
where $\hat{\phi}_0$, $\hat{\phi}_1$ and $\hat{\phi}_2$ are the same as the triangular case and
$$\hat{\phi}_3^\alpha(x,y)=(\nu_1x+\nu_2y+c)^2-(-\nu_2x+\nu_1y)^2+\alpha\hat{\phi}_1(x,y)\hat{\phi}_2(x,y)$$
with a proper real number α. We use the same F as in the triangular case.

The term $\alpha\hat{\phi}_1\hat{\phi}_2$ with $\alpha\neq 0$ in $\hat{\phi}_3^\alpha$ is essential for the unique representation of approximate solutions when the normal vector on an interface satisfies $|\nu_1|=|\nu_2|$. It is easy to see that

$$-div\left(\kappa\nabla\hat{\phi}_3^\alpha\right)=0,\quad \text{on } T=S_-\cup S_+.$$

Then, the finite element space for a rectangular mesh is

$$\mathcal{W}_h=\left\{p\mid p\in\bigoplus_{T\in\mathcal{T}_h}\mathcal{W}_T,\ \int_e p|_T\,ds=\int_e p|_{T'}\,ds,\ e=\partial T\cap\partial T',\ \int_e p|_T\,ds=0,\ e=\partial T\cap\Gamma\right\}.$$

Then we apply the same algorithm as in Section 3. Firstly, find

$$u_h^f=P_0(f)(F-I_hF).$$

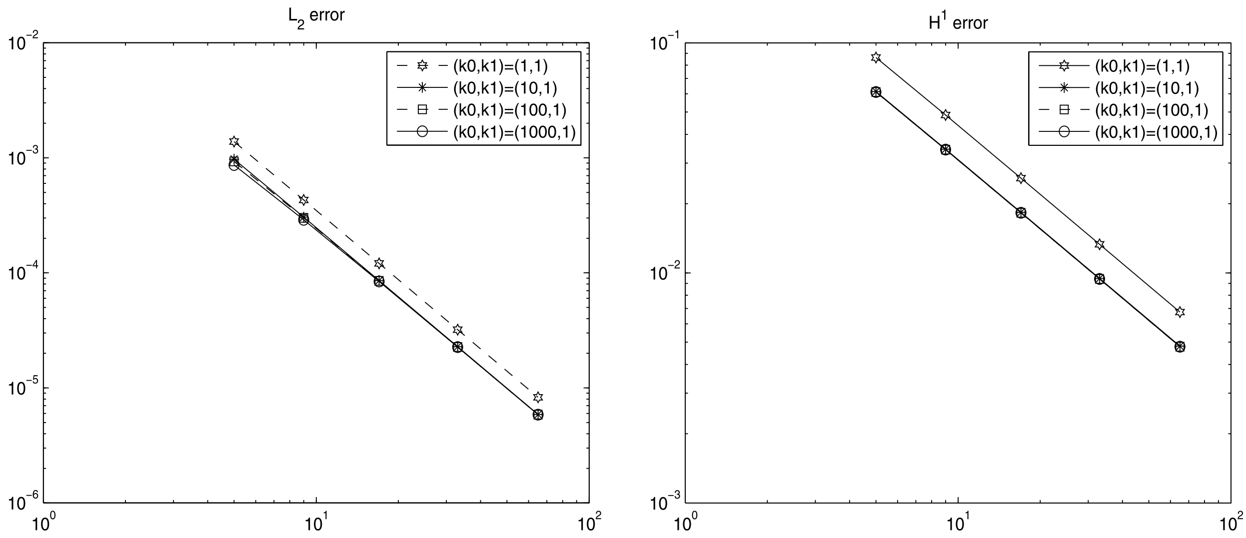

Fig. 3. The L_2 (left) and H^1 (right) errors for rectangular partitions with various conductivity ratio $\tau = 1, 10, 100, 1000$ for Example 6.1.

Step 1: Find $\sigma_h \in \mathcal{W}_h$ that satisfies

$$(\kappa \nabla \sigma_h, \nabla \mu)_h = -\langle [[\kappa \nabla u_h^f]], \overline{\mu} \rangle_{K_h}, \quad \mu \in \mathcal{W}_h.$$

Step 2: Find $V_h \in \prod_{T \in \mathcal{T}_h} \mathcal{W}_T$ up to a constant on each T such that

$$\langle \partial_\nu^\kappa V_h, \overline{\mu} \rangle_{\partial T} = (\kappa \nabla \sigma_h, \nabla \mu)_T, \quad \mu \in \mathcal{W}_h,\ T \in \mathcal{T}_h.$$

The same kind of numerical approximations of u and its flux $\Theta = \kappa \nabla u$ are given as

$$U_h := \sigma_h + u_h^f, \qquad \Theta_h := \kappa \nabla V_h + \kappa \nabla u_h^f.$$

Remark 5.1. Since $\partial_\nu^\kappa v$ is constant on each edge of T for $v \in \mathcal{W}_T$ when T is not an interface rectangle, we have

$$\langle \partial_\nu^\kappa v_h, \overline{\mu} \rangle_{\partial T} = (\kappa \nabla v_h, \nabla \mu)_T, \quad v_h,\ \mu \in \mathcal{W}_h.$$

Therefore, Step 2 is needed only for interface rectangles.

6. Numerical experiments

In this section, we present numerical results on both triangular and rectangular meshes. The computational domain is the unit square $\Omega := [0, 1]^2$ and we consider a uniform mesh so that the vertices are given as $x_i = ih$ and $y_j = jh$, $h = 1/N$ for $1 \leqslant i,\ j \leqslant N$ for the rectangular mesh and the triangular mesh is then generated by bisecting each square by a diagonal line.

Example 6.1. Consider an elliptic problem:

$$-div\,(\kappa \nabla u) = f \quad \text{in } \Omega,$$
$$u = g \quad \text{on } \partial\Omega,$$

where the domain $\Omega = \Omega_- \cup \Omega_+$ with $\Omega_- = [0, \frac{1}{2}] \times [0, 1]$ and $\Omega_+ = [\frac{1}{2}, 1] \times [0, 1]$. The conductivity, κ is piecewise constant so that $\kappa = \kappa_\pm$ on each $\Omega_\pm$. The functions f and g are given so as to have the exact solution:

$$u(x, y) = \begin{cases} \frac{1}{\kappa_-}(x - 1/2)^3 \sin(\pi y), & x \in \Omega_-, \\ \frac{1}{\kappa_+}(x - 1/2)^3 \sin(\pi y), & x \in \Omega_+. \end{cases}$$

We consider both the triangular and rectangular meshes for Example 6.1 and we use the local basis $\{\hat{\phi}_0, \hat{\phi}_1, \hat{\phi}_2, \hat{\phi}_3^0\}$ for the rectangular mesh. Numerical experiments are performed by changing the conductivity ratio $\tau = \frac{\kappa_-}{\kappa_+}$ from 1 to 1000. Remarkably, our numerical method performs quite stably even for a large conductivity ratio. Figs. 3 and 4 represent the

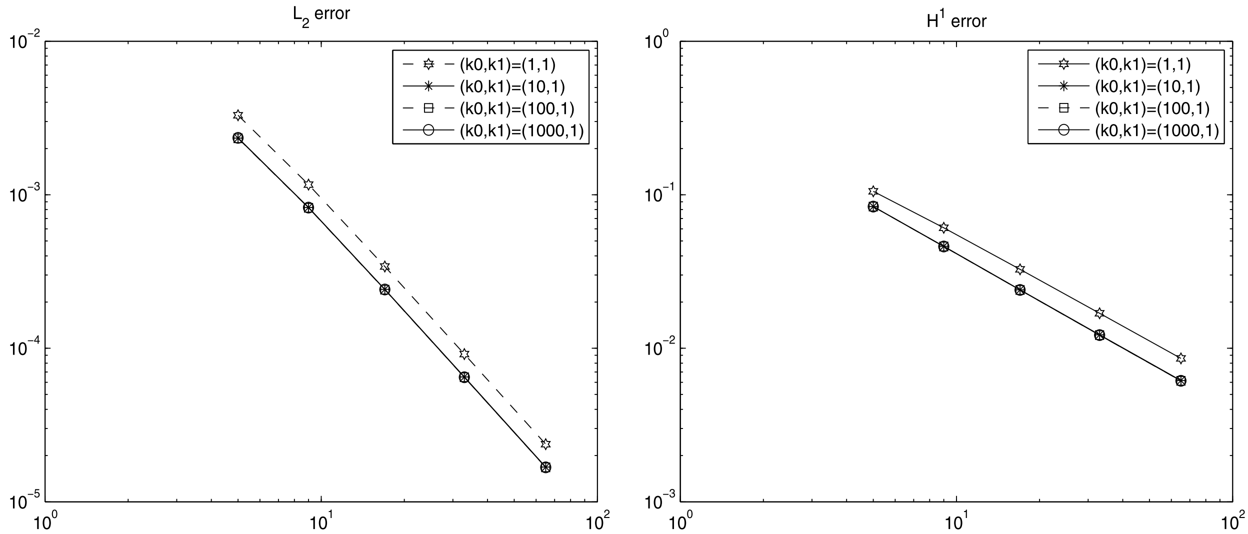

Fig. 4. The L_2 (left) and H^1 (right) errors for triangular partitions with various conductivity ratio $\tau = 1, 10, 100, 1000$ for Example 6.1.

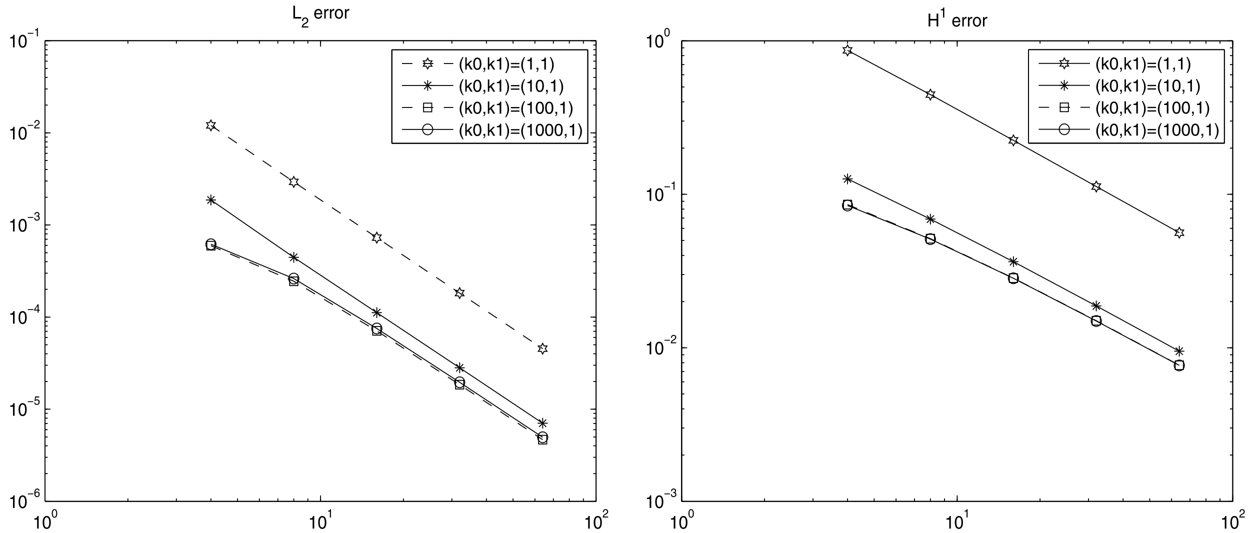

Fig. 5. The L_2 (left) and H^1 (right) errors for rectangular partitions with various conductivity ratio for $\tau = 1, 10, 100, 1000$ for Example 6.2.

L_2 and H^1 errors for Example 6.1 with the rectangular and triangular meshes, respectively. Fig. 5 represents those of Example 6.2 with the rectangular mesh. It is unexpected that the homogeneous conductivity problem yields slightly poor numerics as shown in Figs. 3–5. We observed conservation of the total numerical flux in all numerical experiments.

Example 6.2. Consider the same elliptic problem as in Example 6.1 on the domain $\Omega = \Omega_- \cup \Omega_+$ with $\Omega_- = \{(x, y) \in \Omega\colon\ y > x\}$ and $\Omega_+ = \Omega \setminus \Omega_-$. The exact solution is given as

$$u(x, y) = \begin{cases} \frac{1}{\kappa_-}(e^{x-y} - 1)^2, & x \in \Omega_-, \\ \frac{1}{\kappa_+}(e^{x-y} - 1)^2, & x \in \Omega_+. \end{cases}$$

In this example, we have $\nu_1 = -\nu_2 = \frac{1}{\sqrt{2}}$, therefore, the local rectangular basis $\{\hat{\phi}_0, \hat{\phi}_1, \hat{\phi}_2, \hat{\phi}_3^0\}$ causes instability in the cell average interpolation since

$$\hat{\phi}_3^0(x, y) = 2xy.$$

Therefore, the basis function, $\hat{\phi}_3^0$ must be replaced by $\hat{\phi}_3^\alpha$ with any nonzero α. In this numerical experiment we use $\alpha = 1$.

In all numerical tests we observe that the rates of convergence saturate to the theoretically expected orders as the number of partition increases, that is, the second order and the first order convergence in the L_2 and H^1 norms, respectively. The L_2-convergence analysis is not provided in this paper, however, it will be possible with the standard duality argument. For the rectangular element the choice of α (for ϕ_3^α) must depend on (ν_1, ν_2, c) with the interface equation, $\nu_1 x + \nu_2 y + c = 0$. Apparently, there seems to be no problem if one chooses a nonzero α only when $\nu_1^2 - \nu_2^2 = 0$. More rigorous analysis on this issue will be a subject of further investigation.

References

[1] I. Babuska, G. Caloz, J.E. Osborn, Special finite element methods for a class of second order elliptic problems with rough coefficients, SIAM J. Numer. Anal. 31 (1994) 945–981.

[2] I. Babuska, J. Melenk, The partition of unity method, Int. J. Numer. Methods Eng. 40 (1997) 727–758.

[3] I. Babuska, J.E. Osborn, Finite element methods for the solution of problems with rough input data, in: Singularities and Constructive Methods for Their Treatment, in: Lect. Notes Math., vol. 1121, Springer, 1985, pp. 1–18.

[4] J.H. Bramble, J.T. King, A finite element method for interface problems in domains with smooth boundary and interfaces, Adv. Comput. Math. 6 (1996) 109–138.

[5] S.C. Brenner, L.R. Scott, The Mathematical Theory of Finite Element Methods, Springer, 2002.

[6] B. Cockburn, J. Gopalakrishnan, R. Lazarov, Unified hybridization of discontinuous Galerkin, mixed, and continuous Galerkin methods for second order elliptic problems, SIAM J. Numer. Anal. 47 (2009) 1319–1365.

[7] M. Crouzeix, P.A. Raviart, Conforming and nonconforming finite element methods for solving the stationary Stokes equations, RAIRO. Anal. Numér. 7 (1973) 33–75.

[8] R.E. Ewing, Z. Li, T. Lin, Y. Lin, The immersed finite volume element methods for the elliptic interface problems, Math. Comput. Simul. 50 (1999) 63–76.

[9] X.-M. He, T. Lin, Y. Lin, Approximation capability of a bilinear immersed finite element space, Numer. Methods Partial Differ. Equ. 24 (2008) 1265–1300.

[10] X.-M. He, T. Lin, Y. Lin, A bilinear immersed finite volume element method for the diffusion equation with discontinuous coefficients, Commun. Comput. Phys. 6 (2009) 185–202.

[11] Y. Jeon, E.-J. Park, Nonconforming cell boundary element methods for elliptic problems on triangular mesh, Appl. Numer. Math. 58 (2008) 800–814.

[12] Y. Jeon, E.-J. Park, A hybrid discontinuous Galerkin method for elliptic problems, SIAM J. Numer. Anal. 48 (2010) 1968–1983.

[13] J. Kim, D. Kim, H. Choi, An immersed-boundary finite-volume method for simulations of flows in complex geometry, J. Comput. Phys. 171 (2001) 132–150.

[14] D.Y. Kwak, K.T. Wee, K.S. Chang, An analysis of a broken p_1-nonconforming finite element method for interface problems, SIAM J. Numer. Anal. 48 (2010) 2117–2134.

[15] Z. Li, The immersed interface method using a finite element formulation, Appl. Numer. Math. 27 (1998) 256–267.

[16] Z. Li, T. Lin, R.C. Rogers, An immersed finite element space and its approximation capability, Numer. Methods Partial Differ. Equ. 20 (2004) 338–367.

[17] L. Zhan, A. Gerstenberger, X. Wang, W.K. Liu, Immersed finite element method, Comput. Methods Appl. Mech. Eng. 19 (2004) 2051–2067.